Conf-751108--22

UCRL -77156
PREPRINT



LAWRENCE LIVERMORE LABORATORY
University of California/Livermore, California

# INTENSE, PULSED, ION-DIODE SOURCES AND THEIR APPLICATION TO MIRROR MACHINES

D. S. Prono, J. W. Shearer, and R. J. Briggs

November 12, 1975



This paper was prepared for submission to the International Topical Conference on Electron Beam Research and Technology Albuquerque, New Mexico, November 3-5, 1975

# INTENSE, PULSED, ION-DIODE SOURCES AND THEIR APPLICATION TO MIRROR MACHINES*

D. S. Prono, J. W. Shearer, and R. J. Briggs
University of California, Lawrence Livermore Laboratory
Livermore, California 94550

## ABSTRACT

Startup conditions for future mirror fusion experiments require a rapidly formed target plasma of ~0.5 coulomb of ions with energy of 50 to 100 keV. Theory suggests that very intense ion-flux emission satisfying these requirements can be extracted from a pulsed ion diode. Developing such sources would be an ideal CTR application of the high-power, single-shot capability of pulsed power technology. Recent experimental results are reviewed in which ~2 kA/cm$^2$ of $D^+$ at ~50 keV was extracted. In the experiment, an intense relativistic electron beam undergoes many transits through a solid but range-thin anode foil. With each transit the electrons lose energy, causing their trajectories to collapse toward the anode surface. In so doing, the increased space charge extracts an intense ion flux from the anode foil's plasma. Observations are reported on the importance of diode stability. The general agreement between theoretical scaling laws and experimental results are also presented.

*Work performed under the auspices of the U.S. Energy Research and Development Administration under Contract No. W-7405-Eng-48.

# I. INTRODUCTION

Recent theories have indicated that significant ion currents can flow within the diode of a relativistic electron-beam generator. Basically, there are two diode operational modes that yield enhanced ion flow: pinched electron flow[1-3] and a reflex diode with collapsing electron trajectories due to beam energy loss with successive transits of the foil.[4] In the first case, electron flow is prevented by the beam's self-magnetic field; in the latter, electron flow is restricted by the electrostatic fields of a virtual cathode created by the nonpropagating beam. In both cases, the increased electron space charge across the anode surface is neutralized by the extraction of intense ion flow from the anode plasma. This paper presents recent experimental results investigating the second of these intense ion-flux generators. In brief, a relativistic electron-beam (REB) diode (which normally operated at a peak diode voltage of 850 kV and peak electron diode current of 350 kA) was converted to an operational mode of ~50-kV diode voltage and a total diode current of 750 kA, of which 36 kA was $D^+$ ions.

# II. APPLICATION OF ION DIODES TO CTR MAGNETIC MIRROR CONFINEMENT

Intense ion beams from pulsed diodes could be useful in the initial formation of a mirror-confined fusion plasma. As an example, consider the proposed parameters of the next generation confinement experiment, MFX (Mirror Fusion Experiment), shown in Table I.

Table I. MFX Parameters.

| | | | |
|---|---|---|---|
| Central magnetic field | $\sim 20$ kG | $n$ | $\sim 3 \times 10^{13}$ cm$^{-3}$ |
| $\beta$ | $\gtrsim 0.5$ | $T_i$ | $\sim 50$ keV |
| $n\tau$ | $\sim 10^{12}$ | Volume | $\sim 10^5$ cm$^3$ |

This plasma could be maintained by modest currents from long pulse length (or D.C.) neutral beams; however, the "startup" sequence is critical since many low density states of mirror plasmas are not sufficiently stable.[5] A number of possible approaches are being considered at present, such as the creation of a target plasma by laser irradiation of a pellet as being studied in the present Baseball II facility. The attractive feature of the ion diode approach is the short time scale of the ion injection ($\sim$200 ns). Instabilities of the intermediate density and temperature states of the plasma are of little concern with such a fast injection process. In contrast, buildup with D.C. sources requires on the order of a millisecond with the 1500-A, 60-keV sources being considered for MFX.

To begin assessing the feasibility of this alternative startup approach, we performed an experiment to investigate the phenomena of intense ion currents in REB diodes.

## III. THE EXPERIMENT

The REB generator used was the Physics International OWL II machine; a schematic of the experiment is shown in Figure 1. The cathode stalk was hollow to house ion diagnostics. These diagnostics included a radial array of Faraday cups (located at r = 0, 1.5 and 3.0 cm) and a large

Faraday cup located 15 or 25 cm in back of the radial array. Each Faraday-cup collector was equipped with a thermister, which thus gave calorimetric information. The 15- to 25-cm staggered Faraday cup gave ion energy by time-of-flight analysis. A planar circular cathode of 45 $cm^2$ was used; small holes on the cathode allowed ion flow to reach the Faraday-cup calorimeter detectors. The cathode's surface was made of deuterated titanium with a 24% loading ($\sim$1 $D_2$ molecule for every 4 titanium atoms). A "transit-time-isolator," developed by Physics International, enabled Faraday-cup and calorimetric signals to be brought from the cathode even though the cathode was pulsed to a high negative potential. The concentric anode stalk was equipped with two Rogowskii belts to monitor cathode current, one at the anode base and the other 1 cm from the anode foil. In all cases, both Rogowskii belts gave equal readings, indicating no cathode shank emission.

The circular anode foils (102 $cm^2$) were of varying material and thickness: 1- and 0.5-mil titanium (11.4 and 5.7 $mg/cm^2$), and 1-, 0.25-, and 0.1-mil aluminized Mylar (3.4, 0.86, and 0.34 $mg/cm^2$). The cathode side of the anode foil was covered with a light layer of pump oil when proton flow was sought, and with a 0.1- to 0.2-mil layer of $CD_2$ (deuterated polyethelene) when a deuterium ion current was desired. In the latter case, the deuterium ions accelerated onto the deuterated cathode surface furnished a D-D reaction yielding neutrons. These neutrons were detected externally by a geiger tube and a silver-activated scintillation counter, thereby furnishing another means of diagnosing ion flux. Downstream of the anode foil was a circular metallic drift tube in which the virtual cathode was formed; this drift tube, 1 m long by 177 $cm^2$, was in contact with the anode extension near the anode foil location. External field coils supplied a uniform 16-kG field over the entire anode-cathode extension and also along the drift tube.

Three key features uniquely characterize this experimental arrangement from other similar experiments. First, the ion diagnostics are located in the diode, not downstream of the anode. This is critical because with a virtual cathode, the electron flow is asymmetric. That is, there is a high electron flow from the real cathode to anode, but no net electron flow from the virtual cathode to anode--this asymmetry also affects ion flow. Second, the function of the long drift tube is that no physical barrier should be within several diameters of the anode, else the field topology is altered and a virtual cathode will not be formed. Third, the high currents ($\gtrsim$750 kA) flowing from the cathode produce a self-field of $\sim$40 kG on beam edge, and this field is only partially balanced by the externally applied 16 kG field. Therefore, the experiment was midway between a pinched-flow mode and an axially uniform flow.

It is important to summarize our basic diagnostics:

1) The total diode current, $I_D$, was monitored by Rogowskii belts.
2) The tube voltage, $V_T$, was detected by a capacitive voltage monitor.
3) The time derivative of the net diode current was sensed by a nonintegrated induction loop giving a $\dot{B}_\theta$ signal; this signal was electronically added to $V_T$ to give the "corrected diode voltage," $V_c$.
4) $V_c$, the actual voltage appearing across the diode, is the tube voltage minus the inductive component ($V_c = V_T - L\dot{I}_D = V_T - K\dot{B}_\theta$, where K is a constant depending on geometry).
5) The neutron diagnostics determine total deuterium current flow.

6) The calorimeters give total energy onto the cathode Faraday-cup collectors.

7) The radial array of Faraday cups gives ion-current density (current through small holes in the cathode) as a function of radius.

8) The axially staggered Faraday cup gives ion energy (by time-of-flight), which is compared to $V_c$.

## IV. EXPERIMENTAL RESULTS

The essence of the experiment was to observe diode behavior and ion flow as a function of foil thickness when a virtual cathode is present. The theory proposed in Ref. 4 indicates that when the foil thickness decreases, the average number of transits, $\eta$, that a beam electron makes through the anode foil should increase. Increases in $\eta$ thus cause an increase in electron space charge across the anode and correspondingly increase both electron and ion current. The average number of anode transits is defined as

$$\eta = \frac{1}{\rho\tau}\left(\frac{R}{3}\right) , \qquad (1)$$

where $\rho$ is the anode density, $\tau$ is the anode foil thickness, and R is the residual range.[6] The 1/3 factor is suggested by the data of Ref. 6 as being the correction required to convert residual range into a median range.

In Figure 2 we show how diode characteristics, $I_D$ and $V_c$, change when a virtual cathode is present and the anode foil thickness is varied. Infinite anode thickness implies a condition where $\eta = 1$ (i.e., normal diode behavior). We note that there is a general increase in diode current and decrease in diode voltage. Figures 3a and 3b show actual oscilloscope traces of $I_D$, $V_c$, and Faraday-cup signals for cases of anode foil being 0.5-mil titanium with a pump oil coating ($H^+$ ion flow) and 0.1-mil aluminized Mylar with a $CD_2$ coating ($D^+$ ion flow). The "r = 1.5 cm Faraday cup" signal comes from the sensor located directly behind the cathode plate; "staggered Faraday cup" signals come from the sensor that is 25 cm behind the "r = 1.5 cm" detector. Important points to note on these traces are:

1) There is a 40- to 50-ns early transition phase during which the diode behaves normally. The termination of this transition is marked by a sharp drop in $V_c$ and an increase in the slope of $I_D$. The transition phase is that time required to deposit sufficient energy into the anode foil such that the anode plasma can freely supply space-charge-limited ion flow.
2) Following the transition period, $V_c$ remains roughly constant at a value that is characteristic of foil thickness.
3) Ion flow initiates at the termination of the transition phase.
4) Energy analysis (assuming appropriate $H^+$ or $D^+$ species) of the time-of-flight between "near" and "far" Faraday cups gives ion energy in good agreement with $V_c$.
5) There is structure on the Faraday cup signals which probably results from energy modulation apparent on $V_c$ and/or heavy ion impurities. At this time our diagnostics cannot discriminate between these two possibilities.

The data of Figure 2 is compared to the theory (Ref. 4) in Figure 4. $J_e$, the electron-current density, was determined as $(I_D - I_+)/A$, where $I_D$ is the observed peak total diode current, $I_+$ is the measured ion current, and A is the 45-$cm^2$ cathode area (we assume uniform flow). $J_0$, the oscilloscope traces of $I_D$, $V_c$, and Faraday-cup signals for cases of anode foil being 0.5-mil titanium with a pump oil coating ($H^+$ ion flow) and 0.1-mil aluminized Mylar with a $CO_2$ coating ($D^+$ ion flow). The "r = 1.5 cm Faraday cup" signal comes from the sensor located directly behind the cathode plate; "staggered Faraday cup" signals come from the sensor that is 25 cm behind the "r = 1.5 cm" detector. Important points to note on these traces are:

1) There is a 40- to 50-ns early transition phase during which the diode behaves normally. The termination of this transition is marked by a sharp drop in $V_c$ and an increase in the slope of $I_D$. The transition phase is that time required to deposit sufficient energy into the anode foil such that the anode plasma can freely supply space-charge-limited ion flow.
2) Following the transition period, $V_c$ remains roughly constant at a value that is characteristic of foil thickness.
3) Ion flow initiates at the termination of the transition phase.
4) Energy analysis (assuming appropriate $H^+$ or $D^+$ species) of the time-of-flight between "near" and "far" Faraday cups gives ion energy in good agreement with $V_c$.
5) There is structure on the Faraday cup signals which probably results from energy modulation apparent on $V_c$ and/or heavy ion impurities. At this time our diagnostics cannot discriminate between these two possibilities.

The data of Figure 2 is compared to the theory (Ref. 4) in Figure 4. $J_e$, the electron-current density, was determined as $(I_D - I_+)/A$, where $I_D$ is the observed peak total diode current, $I_+$ is the measured ion current, and A is the 45-cm$^2$ cathode area (we assume uniform flow). $J_0$, the

Child-Langmuire current, was calculated using the average $V_c$ value after the transition phase and assuming a gap spacing 0.5 times the initial A-K gap of 0.95 cm (the 0.5 factor accounts for diode closure). If we assume a likely energy spectrum of the reflected electrons within the diode gap, the theory in Ref. 4 suggests a $J_e/J_0$ vs. $\eta$ dependence shown as the solid line in Figure 4. The dashed lines encircle data points characterizing machine performance for a given foil thickness. For low $\eta$ values there is a large discrepancy between theory and experiment. At present, we believe this discrepancy is due to an over-simplified theoretical model. One possible modification is that whereas the theoretical model is based on a continuous electron energy spectrum extending from zero to full diode voltage, in reality the spectrum is probably truncated at both extremes. However, as the simplified theory suggests, the data shows a pronounced steeping of $J_e/J_0$ vs. $\eta$ as $\eta$ approaches a critical value.

Ion-current density dependence on $\eta'$ is shown in Figure 5. Conditions of $H^+$ and $D^+$ ion flow are denoted by different symbols. Again, the dashed lines encircle data for a given foil thickness; however, this time the 0.5-mil titanium and 0.25-mil aluminized Mylar shots are divided into an upper and lower region. The lower regions characterized ion flow when diode instability was present. Experimentally, the observed features of diode instability were:

1) Diode voltage, $V_c$, showed h.f. oscillations in the 100- to 300-MHz band.

2) The oscillation frequency was correlated to anode foil thickness ($f \propto \frac{1}{\tau}$).

3) Intense ion flow only occurred when h.f. oscillations were quiescent.

4) The ion flux detected during the instability showed severe energy modulation (the staggered time-of-flight Faraday cup showed a temporally broadened pulse).

Diode instability occurred whenever the virtual cathode was formed in vacuum, regardless of foil materials (although for thicker foils with low $\eta$ values, the instability was less pronounced). In retrospect, diode instability for vacuum diodes should have been anticipated.[7] Experimentally, we found that significant suppression of the instability occurred when the virtual cathode was formed in a very low pressure gas ($\sim$20 microns of hydrogen). The gas pressure cannot be higher because then the beam ionization time would be short compared to pulse length (i.e., the virtual cathode would be "shorted out" by the plasma and beam propagation would result). We do not understand at present why a slight gas fill around the virtual cathode causes stabilization, but one possible effect is that a virtual cathode partially neutralized by ions would be less likely to exhibit fast spatial fluctuations.

For conditions where $CD_2$ coated the cathode side of the anode foil, we are able to compare the measurements of ion flow as given by Faraday-cup, calorimetry, and neutron diagnostics. This comparison is given below in Table II. The effective area assumed for deducing ion current density from the neutron count was 30 cm$^2$, and an ion pulse duration of 30 ns was used. Because of the anode debris blow-off, the calorimeters usually give abnormally high signals, but for the thinnest foils used this effect was less pronounced. In general, the agreement between the various diagnostics is within a factor of 2. However, the neutron count estimates are still very preliminary and have a large possible error.

Table II. Comparison of Diagnostics Measuring $D^+$ Current Density.

| | $A/cm^2$ as diagnosed by | | |
|---|---|---|---|
| Anode foil | Faraday cup | Neutron detection | Calorimeter |
| 0.5 -mil Ti | 15 | 25 | -- |
| 0.5 -mil Ti | 30 | 52 | -- |
| 1 -mil Mylar | 140 | 98 | -- |
| 0.25-mil Mylar | 460 | 340 | -- |
| 0.1 -mil Mylar | 1150 | 900 to 1280 | 3380 |
| 0.1 -mil Mylar | 1380 | 850 to 1206 | 2230 |

A final aspect of the experimental results was that the ion-current density, as diagnosed by the radial array of Faraday cups immediately behind the cathode, was observed to be annular, not uniform. For thicker foils, whether the virtual cathode was in vacuum or gas, the Faraday cup at 1.5-cm radius read 2 to 5 times higher than the $r = 0$ or $r = 3$ cm cups. For the thinnest foils, this degree of nonuniformity increased to more than an order of magnitude. Again, we do not have a complete explanation for this observation, but some possible candidates are as follows. Perhaps our electron-current emission across the cathode was not uniform but peaked at larger radii due to electrons emitted along the cathode shank and carried into the diode region along $B_z$ lines. The partial pinching due to high self-fields would thus cause the peak electron fluence to be located at some radius less than the cathode radius. An analogue to this condition would be electron flow from a hollow cathode. A second possible explanation involves a partially pinched but uniform beam and return-current heating of the anode plamsa. If ions are emitted only from that area of the anode plasma that has been sufficiently heated by radial return currents, then the optimum region of heating would be at the radius of the partial pinch and not in the center or at the cathode radius.

## V. SUMMARY AND CONCLUSIONS

In our experiment, an REB diode was made to operate in an extremely low-voltage, high-current mode. Electron currents in excess of 80 times Childs-law current (space-charge-limited flow) were observed. Deuterium currents densities of 0.05 $J_e$ were monitored; this exceeds by a factor of 3 the normal Langmuir value of 0.0165 $J_e$. Although this is only a modest increase, we feel that more serious attention to anode-foil fabrication will minimize impurities causing heavy ion currents and significantly increase $D^+$ flow. Having already achieved $D^+$ current densities > 1 kA/cm$^2$ is in itself a promising step.

The qualitative features of simple theory[4] have been substantiated. Both electron and ion flow increase sharply as $\eta$ approaches a critical value. A disruptive diode instability that quenches ion flow was observed and found to be stabilized by adding low-pressure gas in the virtual cathode region. Why the presence of this gas and its associated tenuous plasma afford stabilization is not known. Equally unexplained is the annular radial profile of ion flow.

## ACKNOWLEDGMENT

We gratefully acknowledge numerous staff members of Physics International Company, whose advice and assistance contributed greatly to this experiment.

## REFERENCES

1. J. W. Poukey, Appl. Phys. Lett. 26, 145 (1975).
2. S. A. Goldstein and R. Lee, Phys. Rev. Lett. 35, 1079 (1975).
3. S. A. Goldstein and J. Guillory, Phys. Rev. Lett. 35, 1160 (1975).
4. D. S. Prono, J. M. Creedon, I. Smith, and N. Bergstrom, J. Appl. Phys. 46, 3310 (1975). See also earlier work on reflex triodes by S. Humphries, Jr. et al., J. Appl. Phys. 46, 137 (1975).
5. J. H. Foote, Instability-Threshold Data from the Baseball II Vacuum Buildup Experiment, Lawrence Livermore Laboratory Rept. UCID-16664 (1974).
6. S. M. Seltzer and M. J. Berger, Nuclear Inst. and Methods 119, 157 (1974).
7. C. K. Birdsall and W. B. Bridges, Electron Dynamics of Diode Regions (Academic Press, New York, 1966), pp. 68-118.

# FIGURE CAPTIONS

Figure 1: Schematic of experimental arrangement as described in the text. Components are: 1) cathode stalk, 2) anode stalk, 3) Rogowskii belts, 4) anode foil, 5) deuterated-titanium cathode tip with small holes to pass ion flow, 6) radially located Faraday cups with calorimeters, 7) axially staggered Faraday cup with calorimeter, 8) drift tube, 9) external $B_z$ coils, and 10) transit time isolator.

Figure 2: Characteristic diode voltage and current caused by variations of anode foil thickness when a virtual cathode is formed.

Figure 3a: Oscilloscope waveforms of diode current, diode voltage, $r = 1.5$ cm Faraday cup, and staggered Faraday cup. The anode foil is 0.5-mil titanium coated with pump oil for $H^+$ emission. The drift tube is filled with $\sim$20 microns of hydrogen.

Figure 3b: Oscilloscope waveforms of diode current, diode voltage, $r = 1.5$ cm Faraday cup, and staggered Faraday cup. The anode foil is 0.1-mil aluminized Mylar coated with $CD_2$ for $D^+$ emission. The drift tube is filled with $\sim$20 microns of hydrogen.

Figure 4: $J_e/J_0$ vs. $\eta$. The dashed lines enclose data points characterizing equal thickness foils and the solid curve is from the simple theory given in Ref. 4.

Figure 5: Ion-current density, $J_i$, vs. $\eta$. Anode foils covered with pump oil yielding $H^+$ emission are denoted by · data points; anode foils covered with $CD_2$ for $D^+$ emission are denoted by o data

points. Dashed lines again enclose data for anode foils of equal thickness, but here we indicate which shots were with the virtual cathode in vacuum, resulting in diode instability.

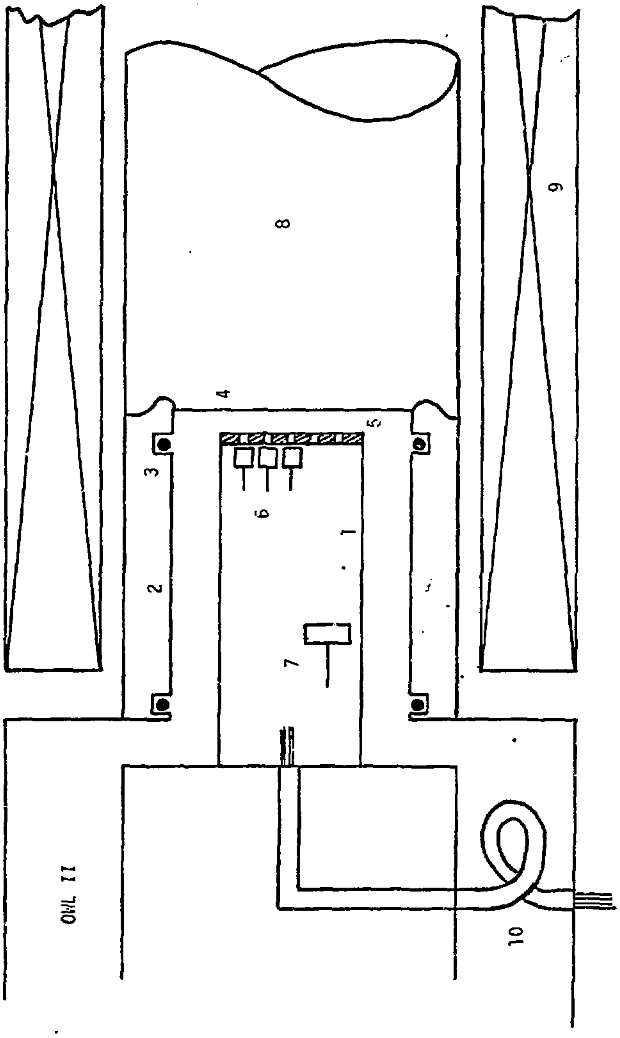


Figure 1

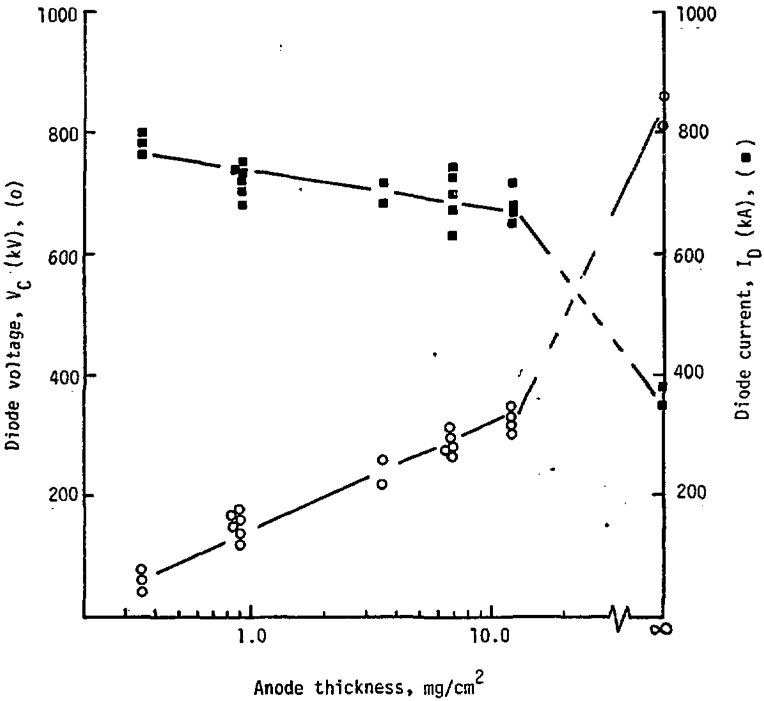
1000
800
600
400
200
Diode voltage, $V_C$ (kV), (o)
1000
800
600
400
200
Diode current, $I_D$ (kA), (■)
1.0
10.0
∞
Anode thickness, mg/cm$^2$

Figure 2

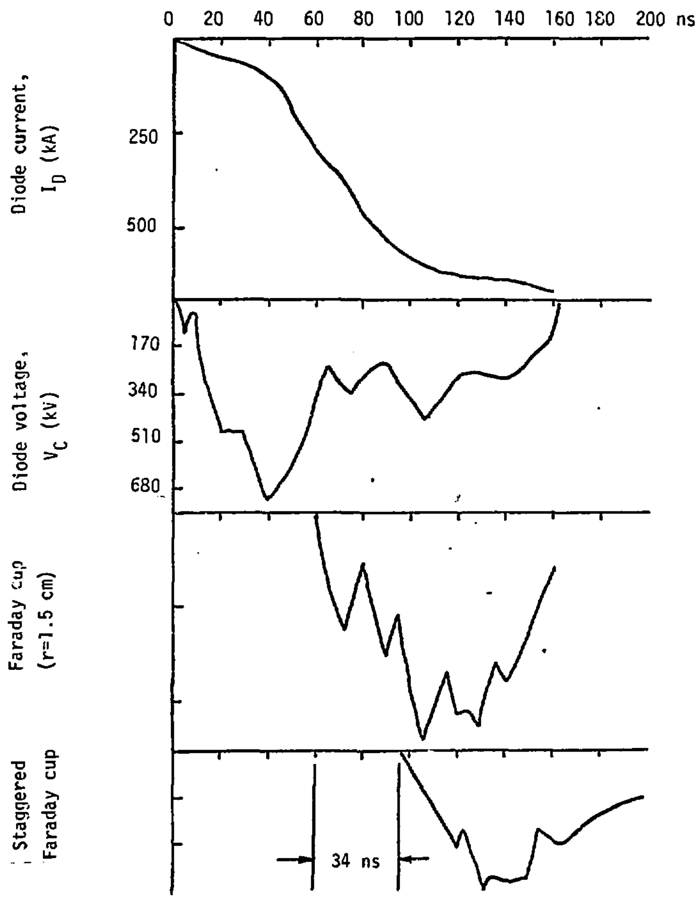
0 20 40 60 80 100 120 140 160 180 200 ns
Diode current,
$I_D$ (kA)
250
500
Diode voltage,
$V_C$ (kV)
170
340
510
680
Faraday cup
(r=1.5 cm)
Staggered
Faraday cup
34 ns

Figure 3a

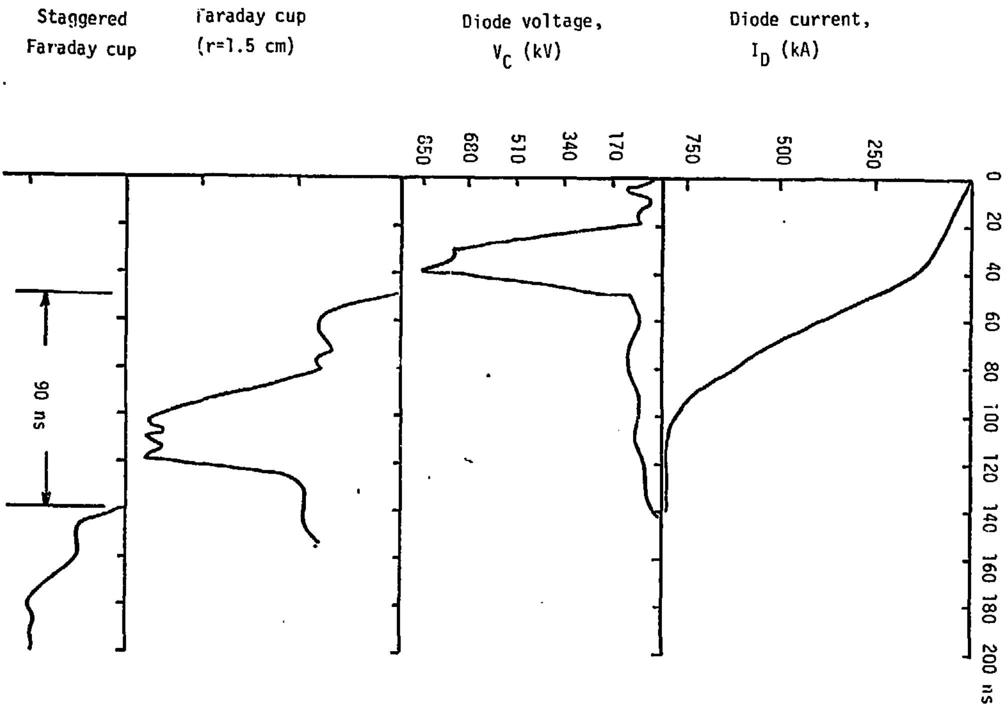
Staggered Faraday cup
Faraday cup (r=1.5 cm)
Diode voltage, V_C (kV)
Diode current, I_D (kA)
850
680
510
340
170
750
500
250
0
20
40
60
80
100
120
140
160
180
200 ns
90 ns

Figure 3b

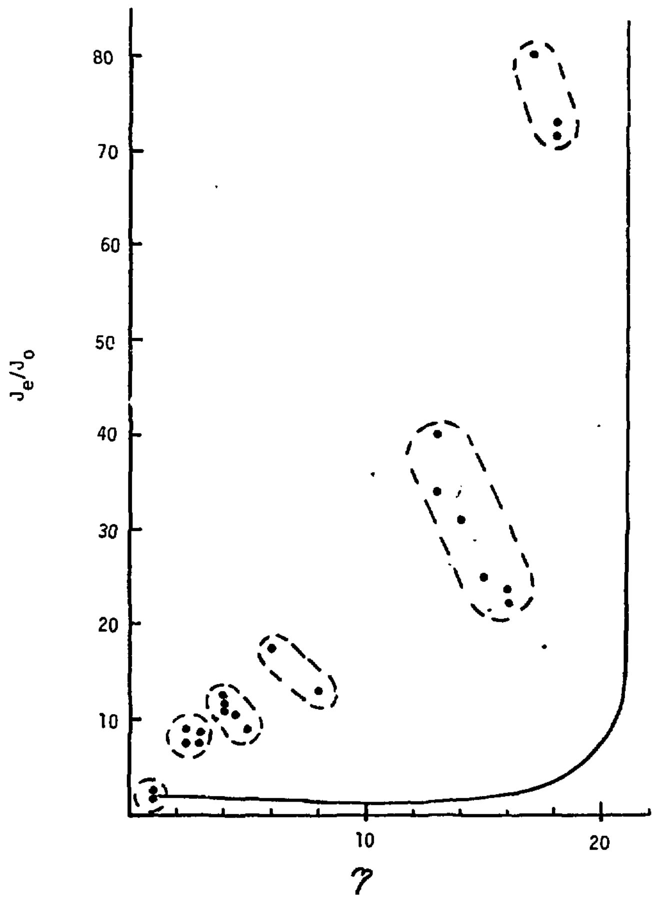


Figure 4

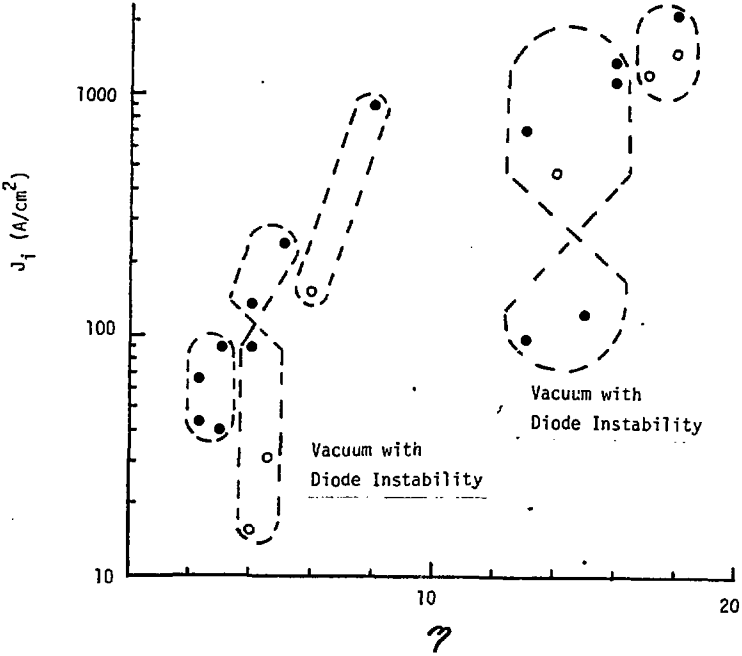
1000
100
10
$J_i$ (A/cm$^2$)
10
20
$\eta$
Vacuum with
Diode Instability
Vacuum with
Diode Instability

Figure 5